Protein Engineering vol.10 no.1 pp.53–61, 1997

Influence of mutations of Val226 on the catalytic rate of haloalkane dehalogenase

Joost P.Schanstra, Anja Ridder, Jaap Kingma and Dick B.Janssen[1]

Department of Biochemistry, Groningen Biomolecular Sciences and Biotechnology Institute, University of Groningen, Nijenborgh 4, 9747 AG Groningen, The Netherlands

[1]To whom correspondence should be addressed

Haloalkane dehalogenase converts haloalkanes to their corresponding alcohols. The 3D structure, reaction mechanism and kinetic mechanism have been studied. The steady state k_{cat} with 1,2-dichloroethane and 1,2-dibromoethane is limited mainly by the rate of release of the halide ion from the buried active-site cavity. During catalysis, the halogen that is cleaved off (Cl_α) from 1,2-dichloroethane interacts with Trp125 and the Cl_β interacts with Phe172. Both these residues have van der Waals contacts with Val226. To establish the effect of these interactions on catalysis, and in an attempt to change enzyme activity without directly mutating residues involved in catalysis, we mutated Val226 to Gly, Ala and Leu. The Val226Ala and Val226Leu mutants had a 2.5-fold higher catalytic rate for 1,2-dibromoethane than the wild-type enzyme. A pre-steady state kinetic analysis of the Val226Ala mutant enzyme showed that the increase in k_{cat} could be attributed to an increase in the rate of a conformational change that precedes halide release, causing a faster overall rate of halide dissociation. The k_{cat} for 1,2-dichloroethane conversion was not elevated, although the rate of chloride release was also faster than in the wild-type enzyme. This was caused by a 3-fold decrease in the rate of formation of the alkyl-enzyme intermediate for 1,2-dichloroethane. Val226 seems to contribute to leaving group (Cl_α or Br_α) stabilization via Trp125, and can influence halide release and substrate binding via an interaction with Phe172. These studies indicate that wild-type haloalkane dehalogenase is optimized for 1,2-dichloroethane, although 1,2-dibromoethane is a better substrate.

Keywords: conformational change/haloalkane dehalogenase/pre-steady state kinetics/product export/protein engineering

Introduction

Haloalkane dehalogenase is one of the few enzymes with a known 3D structure involved in the biodegradation of xenobiotic compounds (Verschueren *et al.*, 1993a). Furthermore, the reaction and kinetic mechanism of the enzyme have been studied in detail (Verschueren *et al.*, 1993b; Pries *et al.*, 1994a, 1995; Schanstra *et al.*, 1996a). The *Xanthobacter autotrophicus* strain expressing haloalkane dehalogenase is used for bioremediation of groundwater polluted with the 'natural' substrate 1,2-dichloroethane (Stucki and Thüer, 1995). Although applicable in these systems, improvement of the catalytic performance and expanding the substrate range of the organism would increase the feasibility of such techniques for bioremediation purposes.

The dehalogenase reaction is initiated by binding of the substrate in the Michaelis complex, followed by nucleophilic attack of Asp124 on the carbon atom to which the halogen is bound, which leads to the formation of an alkyl-enzyme intermediate (Verschueren *et al.*, 1993b; Pries *et al.*, 1994a). This covalent intermediate is subsequently hydrolyzed by an activated water molecule, with His289 acting as a general base catalyst, leading to enzyme and products (Verschueren *et al.*, 1993b; Pries *et al.*, 1995). Recent studies have shown that halide release occurs after cleavage of the covalent intermediate and alcohol release, and that it is the slowest step in the reaction sequence during the conversion of 1,2-dichloroethane and 1,2-dibromoethane (Schanstra *et al.*, 1996a).

The active-site cavity is buried inside the protein. It is lined with the catalytic triad residues Asp124, His289 and Asp260, as well as four phenylalanines, two tryptophans, two leucines, a valine and a proline (Figure 1; Verschueren *et al.*, 1993a). In the course of the reaction, the substrate also interacts with several of the noncatalytic triad active-site residues. In the Michaelis complex, the chlorine atom (Cl_α), which is cleaved off from 1,2-dichloroethane, is located between the hydrogens bound to the indole nitrogens of Trp125 and Trp175 (Verschueren *et al.*, 1993b). Replacing these two tryptophan residues with Gln reduces both the apparent affinity of the enzyme for substrate and the affinity for halides (Kennes *et al.*, 1995). In the X-ray structure of the wild-type alkyl-enzyme, the halide ion that is cleaved off from the substrate was still found between the two Trp residues, whereas the Cl_β lies in the plane of the Phe172 side chain and may be stabilized by interactions with the hydrogen atoms at the $C_{\delta1}$ and $C_{\varepsilon1}$ of this residue (Verschueren *et al.*, 1993b). Replacing phenylalanine 172 by a tryptophan resulted in a dehalogenase mutant with a lower substrate binding and alkylation rate, indicating possible involvement of this residue in substrate binding and/or transition state stabilization during C–X cleavage (Schanstra *et al.*, 1996b). After hydrolysis of the alkyl-enzyme, the halide ion remains bound between the two active-site Trp residues and no density for the product 2-chloroethanol was observed, indicating that it immediately leaves the active site (Figure 1).

As we have found for the mutation of Trp125 and Phe172 in haloalkane dehalogenase (Kennes *et al.*, 1995; Schanstra *et al.*, 1996b), the mutation of residues involved directly in an enzymatic reaction will, in general, drastically change the specificity and reaction rate (Gerlt, 1994), whereas the mutation of amino acids interacting with these residues can have more subtle effects on the specificity and reactivity. In haloalkane dehalogenase, Val226 is not involved directly in the dehalogenase reaction but has van der Waals contacts with Phe172 and Trp125 ($C_{\gamma2}$ Val226–$N_{\varepsilon1}$ Trp125 3.2 Å; $C_{\gamma1}$ Val226–C_ζ Phe172 3.8 Å; Figure 1). Valine 226 itself is located in the wall of the active-site cavity but does not seem to interact directly with 1,2-dichloroethane during the reaction, except that the $C_{\gamma2}$ may interact with the C_β of the substrate in the Michaelis complex (Verschueren *et al.*, 1993b). Phe172 and Trp125 are both located very close to the

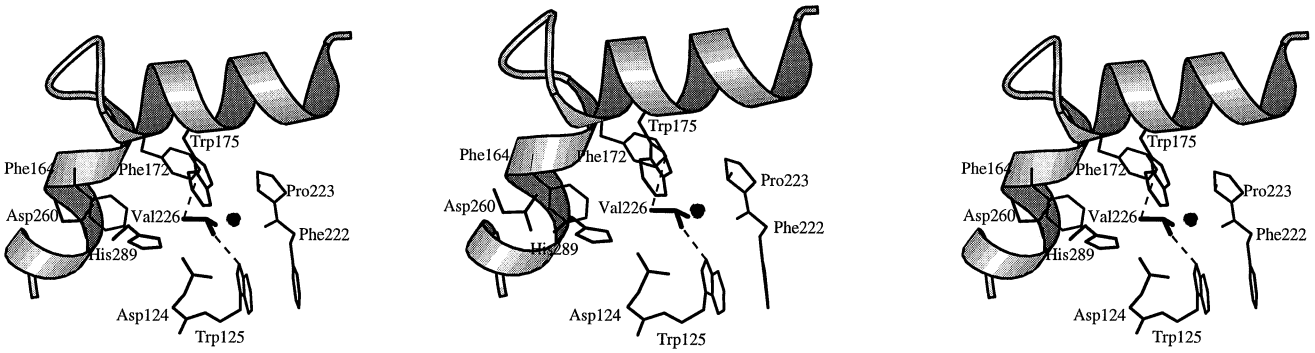

Fig. 1. Stereoscopic representation of the active site of halide-bound haloalkane dehalogenase (pH 6.2, 2 days soaked in 10 mM 1,2-dichloroethane; Verschueren *et al.*, 1993b) with the helix–loop–helix structure. For clarity, Phe128, Leu262 and Leu263 were omitted (drawn using MOLSCRIPT; Kraulis, 1991).

halogen that is cleaved off, and slight changes in their position might thus influence the halide binding site.

To establish the importance of the interactions of Val226 with Trp125 and Phe172, and in an attempt to change the activity of the enzyme without directly mutating catalytic residues, Val226 was mutated to glycine, alanine and leucine. The results show that the addition or removal of one methyl group at the side chain of residue 226 is allowed without extreme changes in the enzyme activity for the natural substrate 1,2-dichloroethane. For 1,2-dibromoethane, however, the Val226Ala and Val226Leu mutants had a 2.5-fold higher catalytic rate than the wild-type enzyme, and a pre-steady state kinetic analysis of the Val226Ala enzyme showed that this could be attributed to more rapid halide release, which was caused by an increased rate of enzyme isomerization that precedes halide dissociation.

Materials and methods

Materials

Halogenated compounds were obtained from Janssen Chimica (Beerse, Belgium) or Merck (Darmstadt, Germany). ^2H_2O (99.8% v/v) was purchased from Merck or Isotec Inc. (Miamisburg, Ohio). The synthetic oligonucleotides were (from 5′ to 3′): pVal226Ala, G***TACGTA***AGTTTCCCAAGATG**GCC**GCGCAACGC, with the *Sna*BI restriction site in bold italic and the mutated codon in bold; pVal226Gly, GTACyGCAAGyTTTCCCAAGATG**GGC**GCGCAACGC, with the mutated codon in bold; and pVal226Leu, GTACGCAAGTTTCCCAAGATG**CTG**GCGCAACGC, with the mutated codon in bold; they were obtained from Eurosequence BV (Groningen, The Netherlands).

Bacterial strains and plasmids

Plasmid pGELAF$^+$, an expression vector based on pET-3d (Studier *et al.*, 1990) with the dehalogenase gene (*dhlA*) under the control of the T7 promoter and an additional f(1)+ origin for the production of single-stranded DNA (Schanstra *et al.*, 1993), was used to overexpress the dehalogenase in *Escherichia coli* strain BL21(DE3) (Studier *et al.*, 1990). *E.coli* strains JM101 (Promega) and BW313 (Kunkel, 1985) were used for the production of single-stranded DNA for sequencing and site-directed mutagenesis, respectively.

DNA manipulations

Standard DNA manipulations were performed as described by Sambrook *et al.* (1989). Mutants were constructed using the method developed by Kunkel (1985). Sequences were confirmed by dideoxy chain termination sequencing (Sanger *et al.*, 1979).

Protein expression and purification

The enzymes were expressed and purified as described previously (Schanstra *et al.*, 1993). For DEAE cellulose chromatography, TEMAG buffer [10 mM Tris–sulfate pH 7.5, 1 mM EDTA, 1 mM 2-mercaptoethanol, 3 mM sodium azide and 10% (v/v) glycerol] was used, while PEMAG buffer [10 mM sodium phosphate, pH 6.0, 1 mM EDTA, 1 mM 2-mercaptoethanol, 3 mM sodium azide and 10% (v/v) glycerol] was used for hydroxylapatite chromatography. The enzyme was concentrated with an Amicon ultrafiltration cell using a PM10 filter and stored in TEMAG at 4°C.

Dehalogenase assays and protein analysis

Dehalogenase assays were performed using the colorimetric detection of halide release as described by Keuning *et al.* (1985). The experimental error of the k_{cat} values was <15%. Protein concentrations were determined with Coomassie brilliant blue using bovine serum albumin as a standard. The concentration of purified enzyme was determined spectrophotometrically using $\varepsilon_{280} = 4.87\times10^4\ M^{-1}\ cm^{-1}$ (Schanstra and Janssen, 1996). Solvent kinetic isotope effects were determined with substrate dissolved in ^2H_2O. Assays were performed as described above using increasing concentrations of ^2H_2O.

The K_m value was determined by measuring alcohol or halide production in 4.5 ml incubations containing various concentrations of the substrate dissolved in 50 mM Tris–sulfate buffer, pH 8.2, and a suitable amount of enzyme. Samples were incubated for 15 min at 30°C. The amount of substrate converted in the incubation period did not exceed 10% of the amount present at the beginning of the experiment. The amount of alcohol produced was determined by gas chromatography. Halide production was determined colorimetrically as described previously (Keuning *et al.*, 1985). K_m values were calculated from the rates of alcohol and halide production by a nonlinear regression analysis using the Michaelis–Menten equation and the program Enzfitter (Leatherbarrow, 1987). The experimental error of the K_m values was <25%.

Pre-steady state kinetic experiments

Stopped-flow fluorescence was used to study the kinetics of halide binding and substrate conversion. The experiments were performed on an Applied Photophysics model SX17MV instrument fitted with a Xe arc lamp with excitation at 290 nm. Fluorescence emission from Trp residues was followed through a 320 nm cut-off filter supplied with the instrument. All reactions were performed at 30°C, and the reported concentrations are those in

the reaction chamber. Each trace shown is the average of three or four individual experiments.

Rapid-quench-flow experiments were performed at 30°C on a rapid-quench-flow instrument (RQF-63) from KinTek Instruments (Johnson, 1992). The experiments were carried out by loading the enzyme in one sample loop (50 µl) and substrate in the second sample loop (50 µl). The reaction was started by rapidly mixing the two reactants and then quenching with 120 µl 0.4 M H_2SO_4 (final concentration) after time intervals ranging from 2 ms to 4 s. The quenched mixture was ejected directly into 1.5 ml ice-cold diethylether containing 0.05 mM 1-bromohexane as the internal standard. After thorough extraction, the diethylether layer was separated from the water layer and neutralized by adding H_2CO_3. The extract was transferred to a 2 ml autosampler vial for automated gas chromatographic analysis. All reported concentrations were in the reaction line of the rapid-quench-flow instrument.

Before stopped-flow fluorescence and rapid-quench experiments, the enzyme was dialyzed for at least 3 h against T_{50}EMA (50 mM Tris–sulfate, pH 8.2, 1 mM EDTA, 1 mM 2-mercaptoethanol and 3 mM sodium azide) or against T_{50}EDA (50 mM Tris–sulfate, pH 8.2, 1 mM EDTA, 1 mM dithiothreitol and 3 mM sodium azide). T_{50}EDA was used for rapid-quench experiments with 1,2-dibromoethane because 2-mercaptoethanol interfered with 2-bromoethanol during gas chromatographic analysis. All halide and substrate solutions were prepared in T_{50}EMA or T_{50}EDA. Halide binding was measured with enzyme dissolved in T_{50}EMAG buffer [T_{50}EMA buffer supplemented with 10% (v/v) glycerol]. Glycerol was added because it improved the reproducibility of the stopped-flow fluorescence transients but did not affect the kinetics of binding. Glycerol (6%) did not affect the binding kinetics of the wild-type enzyme (Schanstra and Janssen, 1996).

Gas chromatography

All samples were analyzed on a Chrompack 438S gas chromatograph equipped with a model 911 autosampler and a CPWax 52 CB column (length, 25 m; diameter, 0.25 mm; Chrompack, Middelburg, The Netherlands), using an ECD detector for the detection of brominated compounds and an FID detector for the detection of chlorinated compounds. The carrier gas was N_2 at 70 kPa. The temperature program was 3 min isothermal at 45°C, followed by an increase to 250°C at a rate of 10°C/min.

Kinetic data analysis

Rapid-quench and stopped-flow fluorescence data were simulated by numerical integration using the computer program Gepasi, designed by P.Mendes (Mendes, 1993; Gepasi for MS-Windows, version 2.0, release 2.08). The Gepasi output was imported into the spreadsheet program Quattro-Pro 5.0 for MS-Windows (Borland international Inc.). Both programs were run simultaneously under MS-Windows on a 486 personal computer.

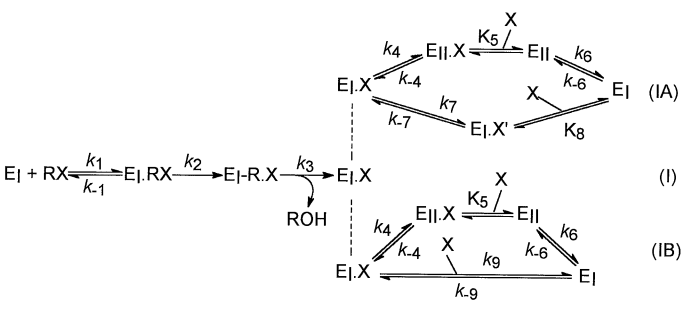

Scheme I.

The complete dehalogenase reaction can be described by Scheme I (IA, bromide; IB, chloride). This is the combined scheme for substrate conversion (Schanstra *et al.*, 1996a) and halide release identified by kinetic studies (Schanstra and Janssen, 1996). For both chloride and bromide, the upper route, starting with k_4, is the most important route for halide release. Its most essential feature is that actual halide release is a rapid equilibrium step (K_5), which is preceded by a slow isomerization step (k_4, or in the case of halide binding k_{-6}), and is followed by a rapid isomerization (k_6, k_{-4} for binding).

In scheme I, both formation (k_2) and hydrolysis (k_3) of the alkyl-enzyme intermediate (E_I–R·X) are considered to be irreversible because no product of the reverse reaction and no inhibition of enzyme activity by alcohol was found (Schanstra *et al.*, 1996a). E_I is the normal native enzyme, whereas E_{II} is the kinetically observed conformational isomer to which halide ions can rapidly bind. E_I·X' is the kinetically observed collision complex in which halide is weakly bound to the native enzyme (Schanstra and Janssen, 1996).

Rate and equilibrium constants for halide binding under pseudo first-order conditions were obtained by numerical simulation of Scheme IA and B. Under these pseudo first-order conditions, the overall rate of halide release (k_{off}), i.e. the rate of conversion of E_I·X to E_I, was extracted from these rate constants by simulation with Gepasi.

Experimental apparent steady state dissociation constants (K_d) for halide binding were determined from the steady state fluorescence levels reached at the end of the stopped-fluorescence transients. Calculation was performed by nonlinear regression fitting in Sigmaplot (version 2.0; Jandel Scientific) of the equation $(F_0 - F)/F_0 = f_a \times [X]/([X] + K_d)$, where F is the observed fluorescence at halide concentration [X], K_d is the apparent dissociation constant and f_a is the fraction of the total fluorescence that is quenched at $[X] >> K_d$. Apparent dissociation constants were also calculated from the kinetic and equilibrium constants given in Scheme IA and B. Using the simplifying assumptions that $k_{-4} >> k_4$ and $k_6 >> k_{-6}$, the apparent dissociation constant determined by fluorescence quenching is given by $K_d = K_8\,[k_7/(k_7 + k_{-7})]$ for Scheme IA and by $K_d = (k_9/k_{-9})$ for Scheme IB.

Rates and equilibrium constants for substrate conversion were derived by numerical simulation of Scheme II (Schanstra *et al.*, 1996a), which is a simplified version of Scheme I.

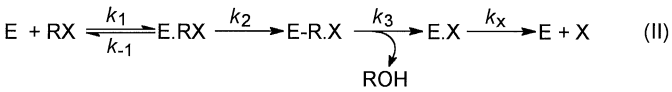

Scheme II.

Under initial velocity steady state conditions,

$$k_{cat} = k_2k_3k_x/(k_2k_3 + k_2k_x + k_3k_x),$$

$$K_m = k_3k_x(k_{-1} + k_2)/(k_1(k_2k_3 + k_2k_x + k_3k_x))$$

and

$$k_{cat}/K_m = k_1k_2/(k_{-1} + k_2).$$

These equations were derived using the determinant method (Huang, 1979). The rate of halide release as determined by a pre-steady state analysis of substrate conversion is depicted by k_x, whereas the rate of halide release as determined from halide binding under pseudo first-order conditions is depicted by k_{off}.

Results

Construction and characterization of the mutant enzymes

The Val226Ala mutant was constructed by Kunkel mutagenesis using wild-type single-stranded DNA as the template. Screening for a Val226Ala mutant was performed by testing for an additional *Sna*BI restriction site which was introduced because it was present in the mutagenic oligonucleotide. The Val226Gly and Val226Leu mutants were obtained by Kunkel mutagenesis using as the template the dehalogenase gene of an inactive deletion mutant (one nucleotide deleted in the codon for Val226) which also carried an additional *Sna*BI restriction site. This mutant was obtained accidentally in the previous mutagenesis round. After mutagenesis, screening for *E.coli* BL21(DE3) transformants producing active dehalogenase was carried out with a pH indicator plate assay and 1,2-dibromoethane as the substrate (Schanstra *et al.*, 1993). Colonies producing active dehalogenase were checked for loss of the *Sna*BI restriction site which was not present in the oligonucleotides used to construct the Val226Gly and Val226Leu mutants.

To examine the effect of the mutation of valine 226 to glycine, alanine and leucine, the activities and Michaelis constants were determined. The mutant and wild-type enzymes were expressed in *E.coli* BL21(DE3) at a temperature of 17°C to avoid expression of the mutant proteins in inclusion bodies. An analysis of the cell-free extracts with SDS–PAGE showed that the expression levels of wild-type and all mutant proteins were similar (Figure 2). The dehalogenase mutant with the highest catalytic activity was Val226Ala (Table I). The specific activity for 1,2-dibromoethane was ~2.5-fold higher in this mutant than in the wild-type enzyme. The Val226Leu mutant had a similar elevated specific activity with 1,2-dibromoethane but a significantly lower activity for 1,2-dichloroethane than the Val226Ala mutant and the wild-type enzyme. The specific activity of the Val226Ala mutant for 1,2-dichloroethane was similar to that of the wild-type enzyme. In all mutants the Michaelis half-saturation constants for both substrates increased. Thus, the addition or removal of one methyl group at the side chain of residue 226 is allowed without extreme changes in enzyme activity. The mutant with the highest activities, Val226Ala, was subjected to a more thorough kinetic analysis.

Steady state kinetic analysis of Val226Ala dehalogenase

Purified enzyme (4 g) was isolated from a 10 l culture of *E.coli* BL21(DE3) expressing the mutant protein. The k_{cat} of the purified Val226Ala enzyme with 1,2-dibromoethane was 2.5-fold higher than that of the wild-type enzyme (Table II), confirming the activity found in cell-free extracts. The k_{cat} of the mutant with 1,2-dichloroethane also seemed to be slightly higher. In addition, the mutant enzyme converted 1-bromo-2-chloroethane 2-fold faster than the wild-type enzyme. This substrate was converted exclusively to 2-chloroethanol, with no indication for the formation of 2-bromoethanol (below the detection limit of the gas chromatograph). However, the Michaelis constants of all three substrates were 1.5- to 3-fold higher than with the wild-type enzyme (Table II).

A clear solvent ^2H_2O kinetic isotope effect on the catalytic rates of both 1,2-dichloroethane and 1,2-dibromoethane conversion was found with the mutant enzyme (Figure 3). This indicates that for both substrates at high substrate concentration the rate-determining step is still at the end of the reaction sequence, as found before with the wild-type enzyme (Schanstra and Janssen, 1996). The conversion of 1-bromo-2-chloroethane also displayed a solvent kinetic isotope effect, in both mutant and wild-type enzyme. To determine why the mutant enzyme had a higher catalytic rate than the wild type with 1,2-dibromoethane but not with 1,2-dichloroethane, the kinetics of substrate conversion in the Val226Ala enzyme were studied using pre-steady state kinetic techniques.

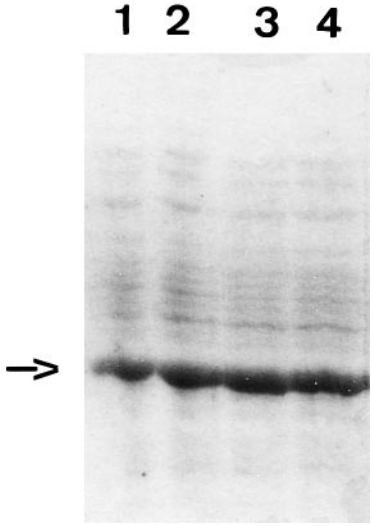

Fig. 2. Expression of wild-type haloalkane dehalogenase and Val226 mutant proteins in cell-free extracts. The haloalkane dehalogenase concentrations in cell-free extracts were estimated by densitometric analysis. Lane 1, 30% wild-type dehalogenase; lane 2, 27% Val226Ala dehalogenase; lane 3, 25% Val226Leu dehalogenase; lane 4, 28% Val226Gly dehalogenase. The arrow indicates the position of haloalkane dehalogenases.

Table I. Specific activities (5 mM substrate) and affinities of wild-type and mutant haloalkane dehalogenase in cell-free extracts of *E.coli* BL21(DE3) transformants

	1,2-Dichloroethane		1,2-Dibromoethane	
	K_m (mM)	Specific activity (U/mg)	K_m (μM)	Specific activity (U/mg)
Val226 (wild type)	0.53	1.7	10	1.2
Val226Gly	>20	0.03	770	1.1
Val226Ala	1.5	1.5	35	2.8
Val226Leu	14	0.22	180	2.9

Pre-steady state kinetic analysis of 1,2-dibromoethane conversion

To identify the rate-determining step(s) in 1,2-dibromoethane conversion by mutant enzyme, a rapid-quench-flow experiment with substrate in excess over enzyme was carried out (Figure 4A). A nearly linear production of 2-bromoethanol in time was observed, indicating that the rate constant of a step preceding hydrolysis of the alkyl-enzyme intermediate or the rate of the hydrolysis step itself was very close to the steady state k_{cat}. The steady state production rate of 2-bromoethanol was 8.3 ± 0.5 s^{-1}, which was identical to the steady state k_{cat} of the mutant enzyme for 1,2-dibromoethane derived from measurements of halide production rates (8.2 s^{-1}; Table II). The slow step was not cleavage of the C–Br bond because, in a single turnover experiment with enzyme in excess (460 μM) over substrate (250 μM), the substrate decrease and product increase curves crossed at 50 μM. This indicated that alkyl-

Table II. Steady state kinetic parameters of purified Val226Ala and wild-type haloalkane dehalogenase

	1,2-Dichloroethane			1,2-Dibromoethane			1-Bromo-2-chloroethane		
	K_m (mM)	k_{cat} (s^{-1})	k_{cat}/K_m (M^{-1} s^{-1})	K_m (mM)	k_{cat} (s^{-1})	k_{cat}/K_m (M^{-1} s^{-1})	K_m (mM)	k_{cat} (s^{-1})	k_{cat}/K_m (M^{-1} s^{-1})
Wild type	0.53	3.3	6.2×10^3	0.010	3.0	3.0×10^5	<0.07[a]	3.2	–
Val226Ala	1.5	3.8	2.5×10^3	0.033	8.2	2.5×10^5	0.097	6.9	7.1×10^4

[a]Lower value could not be measured because of the detection limit of 2-chloroethanol by gas chromatography.

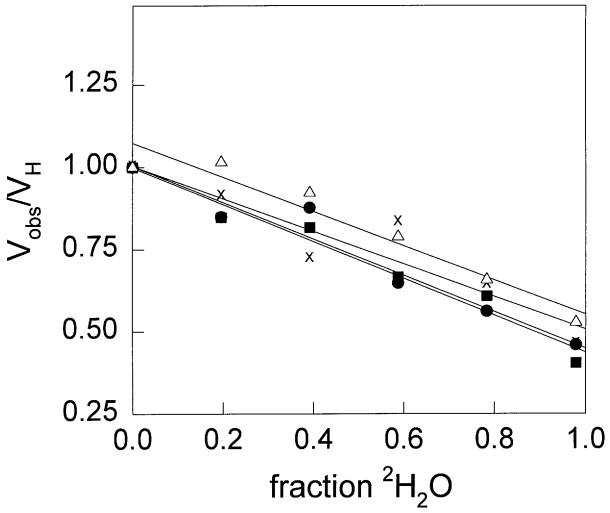

Fig. 3. Solvent ^2H_2O kinetic isotope effects on substrate conversion by Val226Ala and wild-type haloalkane dehalogenase. The observed rate (V_{obs}) as a fraction of the rate observed in ^1H_2O (V_H) was determined at different $^2H_2O/^1H_2O$ ratios for 1,2-dichloroethane (●), 1,2-dibromoethane (■), and 1-bromo-2-chloroethane (Δ) conversion by Val226Ala dehalogenase and for 1-bromo-2-chloroethane (×) conversion by the wild-type enzyme. All substrate concentrations were 5 mM.

enzyme accumulated and the rate of its formation was faster than the rate of hydrolysis (Figure 4B). The slow step must thus be hydrolysis of the alkyl-enzyme intermediate. The higher k_{cat} of the Val226Ala mutant compared with wild-type enzyme was then most probably caused by an increased rate of halide release, which is the main rate-limiting step in the wild-type enzyme. This was studied separately.

The kinetics of bromide binding and release were measured by stopped-flow fluorescence quenching experiments under pseudo first-order conditions. All fluorescence transients obtained in the concentration range 2–800 mM could be fitted by single exponentials (data not shown). To calculate the rate and equilibrium constants for halide binding, the observed binding rate constants (k_{obs}) obtained from the single exponentials were plotted against the bromide concentrations used (Figure 5A). The k_{obs} decreased from 56 s^{-1} at 2 mM KBr to 30 s^{-1} between 25 and 40 mM KBr, followed by an increase in the k_{obs} with an increasing bromide concentration above 40 mM KBr. At bromide concentrations >600 mM, the k_{obs} started to level off somewhat.

As with the wild-type enzyme, this complex dependence of k_{obs} on bromide concentration can be explained by the presence of two parallel routes for bromide binding and release (Scheme IA). The rate and equilibrium constants of this scheme for the Val226Ala enzyme were derived in a similar way to the wild-type enzyme using numerical simulation (Table III). The data indicated that bromide release will mainly follow the upper route of Scheme IA, in which the rate is limited mainly by the unimolecular enzyme isomerization preceding actual release. This step (k_4 in Scheme IA) had a rate of 58 ± 6 s^{-1}. The actual release of the bromide ion is a rapid equilibrium step (K_5, Scheme IA). Compared with the wild-type enzyme, there is a 7-fold faster overall release rate of bromide (k_{off}, Table III), mainly caused by faster enzyme isomerization.

Stopped-flow fluorescence experiments of substrate conversion can provide important information about the rate of substrate entrance because the intrinsic protein fluorescence of the dehalogenase is also partially quenched on binding of the substrate. When excess enzyme was rapidly mixed with 1,2-dibromoethane, a fluorescence progress curve, corresponding to a single enzyme turnover, was obtained (Figure 4C). Doubling the substrate concentration mainly increased the amplitude and rate of the first part of the fluorescence transient, which is related to substrate import and accumulation of the Michaelis complex.

Combination of the steady state and pre-steady state data allowed the extraction of rate constants for the conversion of 1,2-dibromoethane by the Val226Ala mutant (Table IV) using numerical simulation of Scheme II. The steady state k_{cat} and K_m calculated from these rates are close to the values determined experimentally. The slowest step in the conversion of 1,2-dibromoethane was hydrolysis of the alkyl-enzyme, but the rate of this step was similar to that found with wild-type enzyme. The increase in k_{cat} was caused mainly by the increase in the rate of bromide release (k_x), from 4 to 43 s^{-1}. This rate was close to the overall rate of bromide release (k_{off}) found by a stopped-flow analysis of bromide binding under pseudo first-order conditions (Table III).

Pre-steady state analysis of 1,2-dichloroethane conversion

The solvent kinetic isotope effect found on the steady state rate of 1,2-dichloroethane conversion in the Val226Ala mutant (Figure 3) suggested that either hydrolysis of the alkyl-enzyme intermediate or release of the halide ion out of the active-site cavity was rate limiting for this substrate. A stopped-flow fluorescence analysis of chloride binding under pseudo first-order conditions showed that the overall rate of chloride release (k_{off}) in the Val226Ala mutant had increased to 70 s^{-1} (Figure 5B and Table III), which is 5-fold faster than in the wild-type enzyme. The k_{obs} values used to calculate this rate were obtained by fitting fluorescence transients with single exponentials over the complete concentration range (20–800 mM NaCl). The dependence of the k_{obs} on the chloride concentration was similar to that found with the wild-type enzyme (Scheme IB).

From this high rate of chloride release and the solvent kinetic isotope effect on k_{cat}, it was concluded that the slow step in 1,2-dichloroethane conversion is most probably also hydrolysis of the alkyl-enzyme intermediate. If this is true,

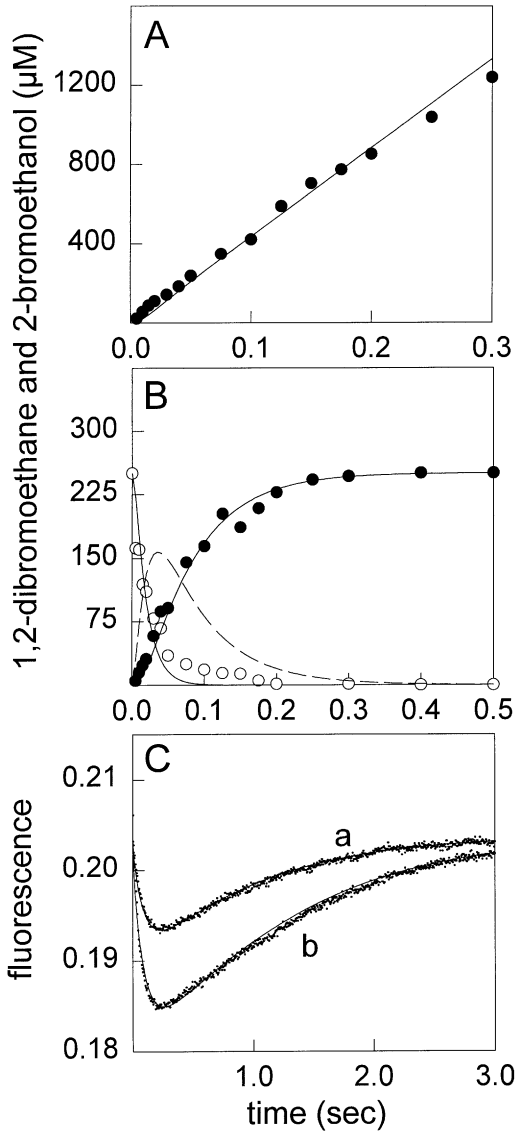

Fig. 4. Rapid-quench and stopped-flow fluorescence analysis of 1,2-dibromoethane conversion by Val226Ala haloalkane dehalogenase. The solid lines are the best fits of the data obtained by simulation of Scheme II using rate and equilibrium constants given in Table IV. (**A**) Experiment in which the production of 2-bromoethanol (●) was followed in time, with 1,2-dibromoethane in excess (10 mM) over enzyme (460 μM). The rate of steady state alcohol production was 8.3 ± 0.5 s^{-1}, as determined from the slope of the plot. (**B**) Single turnover experiment of 1,2-dibromoethane conversion with enzyme (460 μM) in excess over substrate (250 μM), 2-bromoethanol production (●) and 1,2-dibromoethane decrease (○). The dashed line is the simulated concentration of the alkyl-enzyme intermediate (E–R·X) in time. (**C**) Stopped-flow fluorescence analysis of 1,2-dibromoethane conversion. (a) Single turnover with 6 μM enzyme and 5 μM 1,2-dibromoethane; (b) fluorescence transient obtained after mixing 6 μM enzyme with 10 μM 1,2-dibromoethane.

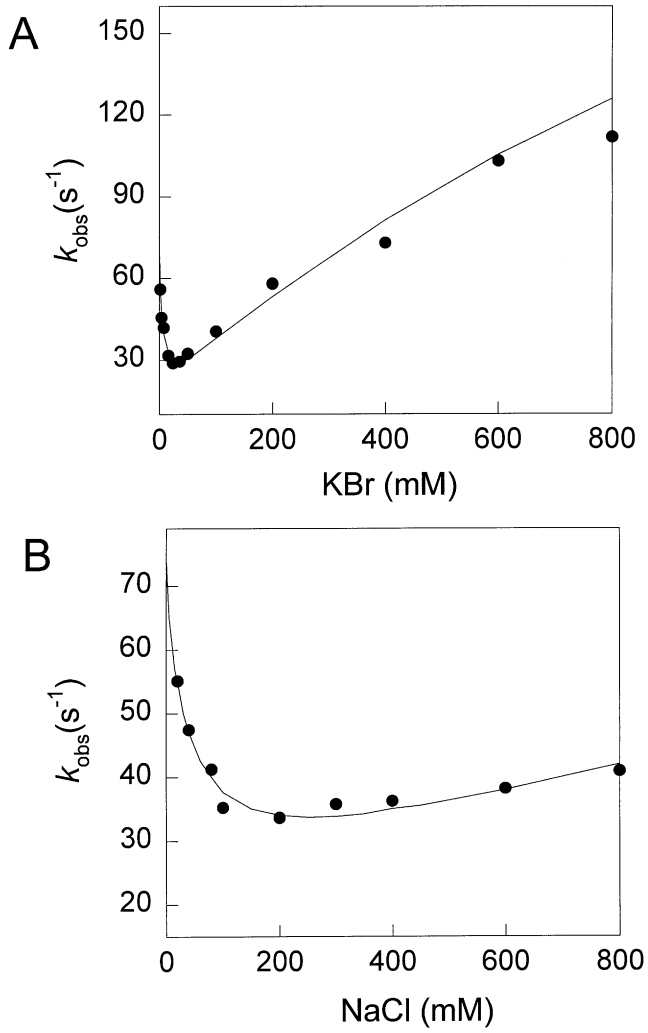

Fig. 5. The kinetics of halide binding under pseudo first-order conditions. (**A**) The dependence of the k_{obs} (●) on bromide concentration obtained from single exponential fits to fluorescence transients of bromide binding (2–800 mM) by Val226Ala haloalkane dehalogenase (6 μM). (**B**) Idem, for chloride binding (●, 20–800 mM) with Val226Ala haloalkane dehalogenase (6 μM). The solid lines are the best fits to Scheme IA and B for bromide and chloride binding, respectively, with equilibrium and rate constants in Table III.

one would expect a lag in alcohol (2-chloroethanol) formation in an experiment with substrate in excess over enzyme. This lag was indeed observed (Figure 6A), but a slow rate of formation of the alkyl-enzyme intermediate and a slow rate of alkyl-enzyme hydrolysis are indistinguishable in such an experiment. A single turnover experiment with enzyme in excess over substrate also provided no discrimination between the two rates in 1,2-dichloroethane conversion in this mutant (Figure 6B) because it is not clear if the slow rate of substrate depletion was caused by a slow association rate of substrate and enzyme or by a slow rate of formation of the alkyl-enzyme intermediate. The lower limit of the rate of association of substrate and enzyme, as set by k_{cat}/K_m (2.5 mM^{-1} s^{-1} for the Val226Ala mutant; Table II; Fersht, 1985; Johnson, 1986), suggested that under single turnover conditions (0.5 mM 1,2-dichloroethane) the rate of substrate binding into the Michaelis complex could be rate limiting. Therefore extra input was necessary from a stopped-flow fluorescence analysis of 1,2-dichloroethane conversion (data not shown). The high K_m for 1,2-dichloroethane allowed only multiple turnover experiments performed at high substrate concentrations (>1.5 mM substrate and 6 μM enzyme). The stopped-flow traces only gave information about the rate of substrate binding (k_1) because no amplitude corresponding to forms of the enzyme occurring after substrate binding was obtained. Based on these stopped-flow experiments, it was concluded that the rate of k_1 was (4.5 ± 1.0) $\times 10^{-3}$ μM^{-1} s^{-1}.

Table III. Rates and equilibrium constants of halide binding to Val226Ala and wild-type haloalkane dehalogenase

	k_4 (s^{-1})	k_{-4} (s^{-1})	k_6 (s^{-1})	k_{-6} (s^{-1})	k_7 (s^{-1})	k_{-7} (s^{-1})	K_8 (mM)	k_9 (s^{-1})	k_{-9} ($mM^{-1}s^{-1}$)	K_d[b] (mM)	K_d calc[c] (mM)	k_{off}[d] (s^{-1})
KBr												
Wild type	9 ± 1	>900	>300	3.0 ± 0.5	0.6 ± 0.1	110 ± 20	1.5 ± 0.6 $\times 10^3$	–[e]	–	10 ± 1	8	9.6
Val226Ala	58 ± 6	>5800	>600	6 ± 2	11 ± 2	350 ± 20	2.2 ± 1.0 $\times 10^3$	–	–	67 ± 8	67	69
NaCl												
Wild type	14.5 ± 0.5	>1450	>300	3.0 ± 0.3	–	–	–	0.66 ± 0.03	8.5 ± 0.5 ($\times 10^{-3}$)	75 ± 5	78	15
Val226Ala	65 ± 5	>6500	>1600	16 ± 3	–	–	–	4.5 ± 0.4	2.4 ± 0.3 ($\times 10^{-2}$)	180 ± 19	188	70

Bromide binding data were obtained by numerical simulation of Scheme IA and chloride binding data by numerical simulation of Scheme IB (see fits in Figure 5)[a].
[a]Wild-type values taken from Schanstra and Janssen (1996).
[b]Experimentally obtained apparent dissociation constant.
[c]Apparent K_d calculated from the obtained rate and equilibrium constants when assuming that the equilibria between E_I [↔] E_{II} and $E_I{\cdot}X$ [↔] $E_{II}{\cdot}X$ in Scheme IA and B are strongly to the left.
[d]Overall halide release rates at [X] = 0 mM (see Materials and methods).
[e](–) Not applicable for scheme used in fit.

Table IV. Haloalkane dehalogenase kinetic constants

	k_1 (μM^{-1} s^{-1})	k_{-1} (s^{-1})	k_2 (s^{-1})	k_3 (s^{-1})	k_x (s^{-1})	k_{cat} calc[b] (s^{-1})	K_m calc[b] (μM)
1,2-Dibromoethane							
Wild-type	0.75 ± 0.10	>20	>130	10 ± 2	4.0 ± 1.5	2.8	4.3
Val226Ala	0.41 ± 0.01	45 ± 10	60 ± 20	12 ± 3	43 ± 10	8.1	35
1,2-Dichloroethane							
Wild type	9 ± 1 ($\times 10^{-3}$)	20 ± 5	50 ± 10	14 ± 3	8 ± 2	4.6	0.72×10^3
Val226Ala	4.5 ± 1 ($\times 10^{-3}$)	25 ± 5	14 ± 1	9 ± 2	50 ± 10	4.9	3.1×10^3

The data given represent the best fit for all of the kinetic and equilibrium data given in this paper[a] (fits in Figures 4 and 6).
[a]Wild-type data are from Schanstra *et al.* (1996a).
[b]The steady state k_{cat} and K_m values calculated from the derived rate constants for a four-step mechanism (Scheme II) (see Materials and methods).

Combination of the steady state and pre-steady state data and numerical simulation of Scheme II yielded a set of rate constants for 1,2-dichloroethane conversion by the Val226Ala mutant (Table IV). The steady state k_{cat} and K_m values calculated from the rates were in agreement with experimentally determined values. As with 1,2-dibromoethane conversion, hydrolysis of the alkyl-enzyme intermediate is the main rate-limiting step during 1,2-dichloroethane conversion by Val226-Ala enzyme (9 s^{-1}). The rates of halide release, as determined by the analysis of substrate conversion (k_x) and by measuring chloride binding under pseudo first-order conditions (k_{off}), were in good agreement. Whereas chloride export had become much faster in the mutant, the rate of C–Cl bond cleavage was reduced from 50 s^{-1} in the wild-type enzyme to 14 s^{-1} in the Val226Ala mutant, resulting in only a small increase in steady state k_{cat}.

Discussion

The mutation of residues involved directly in enzyme catalysis often results in catalytically inactive mutants. This paper describes an analysis of the effect of the mutation of Val226 in haloalkane dehalogenase, the side chain of which interacts with the aromatic ring of the supposed catalytically important residues Trp125 and Phe172.

The properties of the Val226Ala mutant confirmed the observation that halide release is the main rate limiting step in the wild-type enzyme (Schanstra and Janssen, 1996; Schanstra *et al.*, 1996a). Release of the charged halide ion out of the buried active-site cavity occurs via two parallel routes (Scheme IA and B) in both wild-type and mutant enzyme. In the most important route, the actual release is preceded by a slow unimolecular isomerization step (k_4, upper route in Scheme IA and B). An increase in the rate of this isomerization step is the main cause for the faster rate of overall halide release in the Val226Ala mutant compared with the wild-type enzyme. We have hypothesized for the wild-type enzyme that this isomerization is a conformational change of a part of the cap domain of the dehalogenase that is needed to allow water to enter the buried active-site cavity and solvate the halide ion (Schanstra and Janssen, 1996). In the Val226Ala mutant, this proposed conformational change is faster, and therefore Val226 itself, or Trp125 and Phe172, which have van der Waals contacts with Val226 (Figure 1), might have interactions that are lost during this proposed conformational change.

Valine itself seems to interact marginally with substrate and products during 1,2-dichloroethane conversion (Verschueren *et al.*, 1993b). This can contribute to the increase in K_m in the Val226Ala mutant (see below), but cannot explain the increase

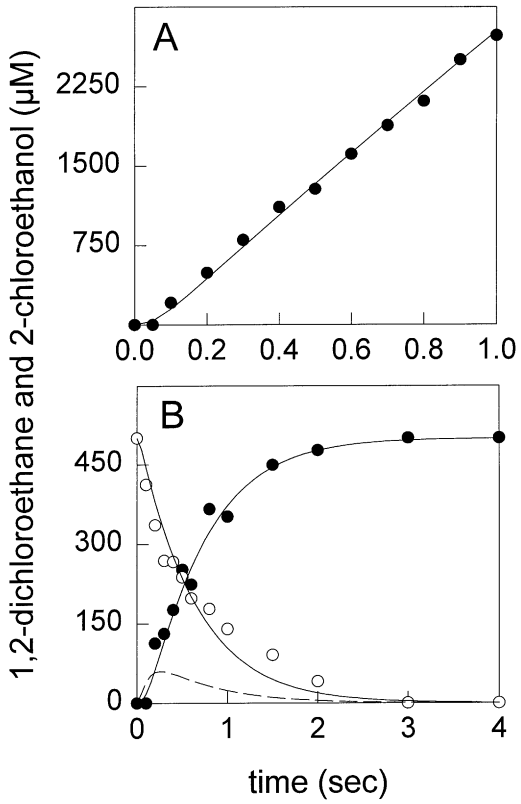

Fig. 6. Rapid-quench-flow analysis of 1,2-dichloroethane conversion by Val226Ala haloalkane dehalogenase. (**A**) Production of 2-chloroethanol (●) after mixing excess 1,2-dichloroethane (11 mM) with haloalkane dehalogenase (740 μM) in the rapid-quench-flow instrument. The steady state alcohol production rate was 3.8 ± 0.2 s^{-1}, as determined from the last part of the graph (0.1–1.0 s). (**B**) Single turnover with enzyme (1.1 mM) in excess over substrate (500 μM), 2-chloroethanol production (●) and 1,2-dichloroethane decrease (○). The dashed line is the simulated concentration of the alkyl-enzyme intermediate (E–R·X) in time. The solid lines are the best fits to the data obtained by simulation with Scheme II using the rate and equilibrium constants given in Table IV.

in the rate of halide release. Trp125 is involved directly in halide binding, in the binding of the halogen moiety of the substrate, and in stabilization of the leaving group during nucleophilic substitution by Asp124 (Verschueren *et al.*, 1993b,c; Kennes *et al.*, 1995). It is, however, not likely that a repositioning of Trp125 caused by the Val226Ala mutation influences the rate of the proposed conformational change because the replacement of Trp125 by phenylalanine resulted in a mutant with a similar k_{cat} for 1,2-dibromoethane to the wild-type enzyme (Kennes *et al.*, 1995). The presence of a solvent kinetic isotope effect showed that the rate-limiting step in this mutant was still at the end of the reaction (Kennes *et al.*, 1995), and stopped-flow fluorescence halide binding studies on this Trp125Phe mutant showed that there was no significant increase in the rate of halide release (G.H.Krooshof, J.J.Schuringa and D.B.Janssen, unpublished data). Thus, it is unlikely that the faster rate of the conformational change in the Val226Ala enzyme is caused by an altered position of Trp125.

Phe172 interacts with the C_α and Cl_β of the substrate during conversion (Verschueren *et al.*, 1993b) and is a member of a helix (H4, 159–166)–loop–helix (H5, 171–181) structure that covers the active site of the dehalogenase and shields it from the solvent (Figure 1). This helix–loop–helix structure is stabilized mainly by a salt bridge (Lys261–Asp170) between the main domain and cap domain of the enzyme, by a hydrogen bond between helices 4 and 5 (Thr173–Val165) and by the hydrophobic interactions of the buried residues Phe161, Phe164 and Phe172 (Pries *et al.*, 1994b). Such buried residues serve as structural anchors and resist translocation (Heinz *et al.*, 1993; Matthews, 1995). Furthermore, Phe172 (H5) and Phe164 (H4) are situated in a tilted-T orientation, where the positive edge of Phe164 can interact with the negative face of Phe172 (Figure 1). Especially in the hydrophobic inside of proteins, such an interaction can contribute to protein stability (Singh and Thornton, 1985; Serrano *et al.*, 1991; Anderson *et al.*, 1993). Furthermore, helices 4 and 5 were found to be 'hot spots' for mutations during the selection of spontaneous haloalkane dehalogenase variants with elevated activity towards longer halogenated alkanes. The elevated activity was attributed to an increased flexibility in this part of the cap domain or an increased size of the active-site cavity (Pries *et al.*, 1994b). Therefore, we propose that the repositioning of Phe172 in the Val226Ala mutant has led to an increase in the flexibility of this part of the cap domain and a faster rate of conformational change that is required for halide release.

Although the most important effect of mutating Val226 was the increased rate of halide release, leading to a higher k_{cat} for 1,2-dibromoethane, other effects were observed. The bimolecular rate constant for the association of substrate and enzyme and the rate of formation of the alkyl-enzyme intermediate decreased in the Val226Ala mutant with both 1,2-dichloroethane and 1,2-dibromoethane. This may be because of an altered interaction of the halogen with Trp125 as this residue directly binds the leaving group (Verschueren *et al.*, 1993b,c; Kennes *et al.*, 1995). Val226 and Phe172 may also be involved in substrate binding by providing a tight hydrophobic cavity, and in transition state stabilization by proper orientation of the R group of the substrate via an interaction with the C_β and Cl_β of the substrate before and during alkylation. This seems to be more important for substrates with a Cl_β than for substrates with a Br_β, as indicated by the intermediate K_m for the substrate 1-bromo-2-chloroethane in both wild-type and mutant dehalogenase. 1-Bromo-2-chloroethane is exclusively converted to 2-chloroethanol.

The Val226Ala mutation did not significantly alter the rate of dealkylation for both 1,2-dichloroethane and 1,2-dibromoethane, indicating that other regions (i.e. His289 activating the nucleophilic water molecule, oxyanion hole) are not significantly altered in the mutant. This 'uncoupling' between the rates of alkylation and dealkylation in haloalkane dehalogenase is allowed because these two processes are not mirror images of each other, unlike acylation and deacylation in the serine proteases.

For both 1,2-dibromoethane and 1,2-dichloroethane, the increase in rate of halide release was accompanied by a reduction in the rate of carbon–halogen bond cleavage, resulting in lower specificity constants. Thus, interactions in the active site of the dehalogenase link an increase in the rate of halide release to a decrease in the rate of substrate binding and carbon–halogen bond cleavage. The kinetic mechanism of the wild-type enzyme appears to be optimized for 1,2-dichloroethane conversion in the sense that there is an optimal balance between the rates of steps that cannot be changed independently (Benner, 1989). 1,2-Dichloroethane is the growth substrate on which the *X.autotrophicus* strain that produces the enzyme was isolated (Janssen *et al.*, 1985). For a substrate such as

1,2-dibromoethane, improvement can obtained by increasing the rate of bromide release, whereas improvement of the kinetic constants for substrates where the rate-limiting step is carbon–halogen bond cleavage (i.e. 1,2-dichloropropane, dichloromethane; Schanstra and Janssen, 1996) can possibly be obtained by decreasing the flexibility of the active-site cavity.

Acknowledgements

We thank Ivo Ridder for providing Figure 1 and Ard Wieringa for experimental assistance. This work was supported by a grant from the Biotechnology Programme of the Dutch Ministry of Economic Affairs.

References

Anderson,E.D., Hurley,J.H., Nicholson,H., Baase,W.A. and Matthews,B.W. (1993) *Protein Sci.*, **2**, 1285–1290.
Benner,S.A. (1989) *Chem. Rev.*, **89**, 789–806.
Fersht,A.R. (1985) *Enzyme Structure and Mechanism* 2nd edition, W.H.Freeman, New York.
Gerlt,J.A. (1994) *Curr. Opin. Struct. Biol.*, **4**, 593–600.
Heinz,D.W., Baase,W.A., Dahlquist,F.W. and Matthews,B.W. (1993) *Nature*, **361**, 561–564.
Huang,C.Y. (1979) *Methods Enzymol.*, **63**, 54–83.
Janssen,D.B., Scheper,A., Dijkhuizen,L. and Witholt,B. (1985) *Appl. Environ. Microbiol.*, **49**, 673–677.
Johnson,K.A. (1986) *Methods Enzymol.*, **134**, 677–705.
Johnson,K.A. (1992) *Enzymes*, **10**, 1–61.
Kennes,C., Pries,F., Krooshof,G.H., Bokma,E., Kingma,J. and Janssen,D.B. (1995) *Eur. J. Biochem.*, **228**, 403–407.
Keuning,S., Janssen,D.B. and Witholt,B. (1985) *J. Bacteriol.*, **163**, 635–639.
Kraulis,P.J. (1991) *J. Appl. Crystal.*, **24**, 946–950.
Kunkel,T.A. (1985) *Proc. Natl Acad. Sci. USA*, **82**, 488–492.
Leatherbarrow,R.J. (1987) *Enzfitter: A Non-Linear Regression Data Analysis Program for the IBM PC*. Elsevier Science Publishers BV, Amsterdam, The Netherlands.
Matthews,B.W. (1995) *Adv. Protein Chem.*, **46**, 249–278.
Mendes,P. (1993) *Comput. Applic. Biosci.*, **9**, 563–571.
Pries,F., Kingma,J., Pentenga,M., van Pouderoyen,G., Jeronimus-Stratingh,C.M., Bruins,A.P. and Janssen,D.B. (1994a) *Biochemistry*, **33**, 1242–1247.
Pries,F., van den Wijngaard,A.J., Bos,R., Pentenga,M. and Janssen,D.B. (1994b) *J. Biol. Chem.*, **269**, 17490–17494.
Pries,F., Kingma,J., Krooshof,G.H., Jeronimus-Stratingh,C.M., Bruins,A.P. and Janssen,D.B. (1995) *J. Biol. Chem.*, **270**, 10405–10411.
Sambrook,J., Fritsch,E.F. and Maniatis,T. (1989) *Molecular Cloning: A Laboratory Manual*. 2nd edition. Cold Spring Harbor Laboratory Press, Cold Spring Harbor, NY.
Sanger,F., Nicklen,S. and Coulsen,A.R. (1979) *Proc. Natl Acad. Sci. USA*, **74**, 5463–5467.
Schanstra,J.P. and Janssen,D.B. (1996) *Biochemistry*, **35**, 5624–5632.
Schanstra,J.P., Rink,R., Pries,F. and Janssen,D.B. (1993) *Protein Express. Purif.*, **4**, 479–489.
Schanstra,J.P., Kingma,J. and Janssen,D.B. (1996a) *J. Biol. Chem.*, **271**, 14747–14753.
Schanstra,J.P., Ridder,I.S., Heimeriks,G.J., Rink,R., Poelarends,G.J., Kalk,K.H., Dijkstra,B.W. and Janssen,D.B. (1996b) *Biochemistry*, **35**, 13186–13195.
Serrano,L., Bycroft,M. and Ferhst,A.R. (1991) *J. Mol. Biol.*, **218**, 465–475.
Singh,J. and Thornton,J.M. (1985) *FEBS Lett.*, **191**, 1–6.
Stucki,G. and Thüer,M. (1995) *Environ. Sci. Technol.*, **29**, 2339–2345.
Studier,F.W., Rosenberg,A.H., Dunn,J.J. and Dubendorff,J.W. (1990) *Methods Enzymol.*, **185**, 60–89.
Verschueren,K.H.G., Franken,S.M., Rozeboom,H.J., Kalk,K.H. and Dijkstra,B.W. (1993a) *J. Mol. Biol.*, **232**, 856–872.
Verschueren,K.H.G., Seljée,F., Rozeboom,H.J., Kalk,K.H. and Dijkstra,B.W. (1993b) *Nature*, **363**, 693–698.
Verschueren,K.H.G., Kingma,J., Rozeboom,H.J., Kalk,K.H., Janssen,D.B. and Dijkstra,B.W. (1993c) *Biochemistry*, **32**, 9031–9037.

Received April 22, 1996; revised September 18, 1996; accepted September 30, 1996